Thermal conductivity and charge imbalance in superconductors

J. Beyer Nielsen
NORDITA, Blegdamsvej 17, DK-2100 Copenhagen Ø, Denmark

H. Smith
Physics Laboratory I, H. C: Ørsted Institute Universitetsparken 5, DK-2100 Copenhagen Ø, Denmark
(Received 31 May 1984)

We use the quasiclassical Green-function formalism to derive kinetic equations describing thermal transport and charge relaxation in superconductors. The effects of pair-breaking processes due to magnetic impurities or phonons are fully included, allowing the case of strong electron-phonon coupling to be considered. We calculate the temperature-dependent thermal conductivity of a superconductor by solving numerically the kinetic equation for the distribution function. In the strong-coupling case we solve in addition the nonlinear Eliashberg equations for the renormalization and gap functions. The resulting thermal conductivity shows a pronounced maximum at low temperatures in the case of pure Pb, and a gradual disappearance of the maximum with increasing amounts of impurity scattering. The charge-relaxation rate in the strong-coupling case shows near T_c the same dependence on the gap function as in the case of weak coupling, but at lower temperatures there are pronounced differences between the temperature dependence of the relaxation rates in the two cases.

I. INTRODUCTION

One of the earliest applications of the BCS theory of superconductivity was the explanation of the temperature dependence of the impurity-limited thermal conductivity in the superconducting state. The ratio between the thermal conductivity in a superconducting metal and that in its normal state at the same temperature was shown by Bardeen *et al.*[1] to obey a universal law, depending only on the ratio between the energy gap Δ and $k_B T$, where T is the temperature. For sufficiently clean materials, the electron-phonon scattering must also be taken into account. This was done by Bardeen *et al.* as well. The inelastic electron-phonon scattering leads to mathematical complications in solving the Boltzmann equation for the distribution function of the BCS quasiparticles, but they are no worse than in the normal metal, where the inelasticity plays an important role at temperatures well below the Debye temperature.

Within the quasiparticle model employed by Bardeen *et al.*, the approach to thermal conduction is straightforward: One needs to consider the modification of the energy spectrum and the associated change of the group velocity in the superconducting state, as well as the coherence factors modifying the normal-state collision probability. The kinetic equation is formulated by separating the driving effect of the temperature gradient from the relaxation due to collisions, as in the conventional Boltzmann approach to transport in dilute gases.

The validity of the Boltzmann equation in normal metals is restricted by the condition $\hbar/\tau \ll \epsilon_F$, when τ is the collision rate and ϵ_F the Fermi energy. The superconducting state is characterized by an energy gap Δ in the excitation spectrum. The criteria for the validity of the Boltzmann-equation approach in the superconducting state depends on the nature of the collisions. For elastic collisions against nonmagnetic impurities with scattering rate $\tau_{\rm imp}^{-1}$ there is no restriction on $\hbar/\tau_{\rm imp}$ compared to Δ, but for inelastic collisions with scattering rate $\tau_{\rm in}^{-1}$, the validity of the quasiparticle Boltzmann equation requires $\hbar/\tau_{\rm in} \ll \Delta$. The inelastic scattering processes broaden the quasiparticle states, and this broadening can only be neglected when the condition $\hbar/\tau_{\rm in} \ll \Delta$ is satisfied. A similar role is played by magnetic impurity scattering. Both the electron-phonon and the magnetic impurity scattering cause pair breaking, which must be taken into account in a self-consistent manner. Ordinary impurity scattering, however, does not change the character of the quasiparticle states under isotropic conditions. In the presence of anisotropy associated with supercurrents or a momentum-dependent gap, the elastic impurity scattering also gives rise to pair breaking and a consequent broadening of the quasiparticle states.

Near the transition temperature T_c, where the energy gap Δ is small, the quasiparticle approach must therefore break down even in weak-coupling superconductors. In materials such as Sn or In the relevant temperature region is very small, of order $\delta T \sim T_c^5/\Theta_D^4$, where Θ_D is the Debye temperature. The effect of collision broadening may be neglected in weak-coupling superconductors, but in strong-coupling materials such as Pb or Hg the effects of pair breaking are much more pronounced.

It is an experimental fact that the temperature dependence of the measured thermal conductivity of pure Pb is very different from that of pure Sn or In. In the case of pure Pb, the slope of the thermal conductivity ratio $\kappa_s(T)/\kappa_N(T)$, as a function of T/T_c, was found experimentally[2] to be approximately 9 near T_c, compared to a slope of 1.6 for Sn.[3] This was explained as being an effect of strong coupling by Ambegaokar and Tewordt,[4] who de-

rived a kinetic equation valid for strong-coupling superconductors, and by Ambegaokar and Woo,[5] who calculated the thermal conductivity in the relaxation time approximation and found a slope of about 11 at T_c.

During the last decade there has been renewed interest in nonequilibrium superconductivity. Most of the attention has focused on phenomena such as charge or gap relaxation, which have no counterpart in normal metals. The use of quasiclassical approximation schemes has proven a powerful tool in establishing kinetic equations of more general validity than the Boltzmann equation. Such an approach was pioneered by Eilenberger,[6] Eliashberg,[7] Larkin and Ovchinnikov,[8] and by Schmid and Schön.[9] The quasiparticle approach has been described by Aronov and Gurevich,[10] by Betbeder-Matibet and Nozières,[11] and by Pethick and Smith.[12]

In this paper we shall reconsider thermal conductivity from the more general quasiclassical point of view. Our aim is to derive and solve kinetic equations describing both charge imbalance and thermal conductivity without making any assumptions on the magnitude of the inelastic scattering rates. We shall also be interested in comparing our approach with the less general one based on the BCS quasiparticle concept, and for that purpose we find it particularly convenient to employ the projection-operator method introduced by Shelankov.[13]

As we shall see, the kinetic equations that describe electronic thermal conductivity and charge imbalance possess identical electron-phonon collision operators at temperatures well below the Debye temperature. Only the driving terms differ in their dependence on energy. The energy-dependent driving terms have opposite parity, as in the case of electrical and thermal conductivity in normal metals. The two properties therefore involve eigenfunctions of the collision operator that are either even or odd with respect to the energy variable.

The kinetic equation derived in the next section is based on a simple spherical approximation for the one-electron energy bands. The effective phonon density of states, $\alpha^2F(\omega)$, however, may exhibit a complicated dependence on frequency ω. This frequency dependence is important in determining the temperature dependence of the thermal conductivity or the charge-relaxation rate. In a Debye model, one has $\alpha^2F \propto \omega^2$, but if low-lying transverse phonons are important, as in the case of Pb, the effective phonon density of states develops considerable structure. Such a frequency dependence has a strong influence on the temperature dependence of the thermal conductivity in the superconducting state. In fact, as we shall see in detail later, most of the pronounced differences between weak- and strong-coupling superconductors are due to the frequency dependence of α^2F, although renormalization and lifetime effects will also contribute to the difference.

The quasiclassical kinetic equation forms a general starting point for realistic calculations of the transport properties of superconducting materials. The mathematical difficulties in solving the kinetic equation are not greater than with the quasiparticle approach. For strong-coupling materials it is, in addition, necessary to solve the nonlinear Eliashberg equation for the frequency dependence of the gap and the renormalization function. Once this equilibrium problem has been tackled, the solution of the kinetic equation proceeds as in the case of weak coupling.

We shall now briefly indicate the connection between the present work and that of previous authors. The charge-relaxation rate was obtained by Tinkham[14] and by Schmid and Schön[9] in the temperature range near T_c where the gap is small compared to k_BT, with electron-phonon scattering as the dominant relaxation mechanism. At lower temperatures, within the BCS quasiparticle approach, the charge-relaxation rate associated with tunnel injection was calculated by Chi and Clarke.[15] Beyer Nielsen *et al.*[16] determined the temperature-dependent rate of charge relaxation by solving the general quasiclassical kinetic equation with pair breaking fully included under conditions where the generation of charge was due to tunnel injection or to the application of a temperature gradient in the presence of superflow.

In the present work we extend these calculations to the strong-coupling case and also consider the thermal conductivity. A brief account of our work has been published previously.[17] Near T_c we find a similar dependence on temperature for the charge-relaxation rate as in the case of weak coupling, but at lower temperatures there are pronounced differences. The thermal conductivity of a pure material depends very differently on temperature in the weak- and strong-coupling case. In the case of pure Pb, we find that the thermal conductivity drops rapidly below T_c but increases again at lower temperatures, showing a pronounced maximum at $T \simeq 0.3T_c$, in qualitative agreement with recent experiments.[18]

In the following sections we derive the kinetic equation from first-principles theory by including different relaxation processes, scattering against ordinary impurities as well as magnetic impurities and electron-phonon scattering. Electron-electron scattering could also be included, but we leave it out of consideration since it is expected to have a negligible effect on our results.

The paper is organized as follows: In the following section we derive the kinetic equations within the quasiclassical approximation, with full account of the pair-breaking processes due to electron-phonon and magnetic impurity scattering. Section III treats the thermal conductivity of weak- and strong-coupling materials and compares the calculated transport coefficients to experiments on Sn and Pb. Finally, Sec. IV contains calculations of charge imbalance and compares the results of the strong-coupling theory to experiments on Pb. Further details of this work, including its generalization to time-dependent situations, are discussed by Beyer Nielsen.[19]

II. DERIVATION OF KINETIC EQUATIONS

The basic ingredient of the microscopic approach to a kinetic equation describing nonequilibrium properties of superconductors is the Nambu Green function, which is a 2×2 matrix representation for Green functions in particle-hole space. The nonequilibrium properties are

conveniently described using a formalism developed by Keldysh,[20] who introduced a further 2×2 matrix representation where the Green functions and self-energies are arranged in the form of matrices,

$$\hat{G}=\begin{bmatrix} G^R & G^K \\ 0 & G^A \end{bmatrix},\quad \hat{\Sigma}=\begin{bmatrix} \Sigma^R & \Sigma^K \\ 0 & \Sigma^A \end{bmatrix}, \tag{2.1}$$

where G^R, G^A, and G^K are matrices in Nambu space and are defined by

$$G^R=G^R(1,2)=-i\Theta(t_1-t_2)\left\langle\begin{bmatrix} [\psi_\uparrow(1),\psi_\uparrow^\dagger(2)]_+ & [\psi_\uparrow(1),\psi_\downarrow(2)]_+ \\ -[\psi_\downarrow^\dagger(1),\psi_\uparrow^\dagger(2)]_+ & -[\psi_\downarrow^\dagger(1),\psi_\downarrow(2)]_+ \end{bmatrix}\right\rangle, \tag{2.2}$$

$$G^A=G^A(1,2)=i\Theta(t_2-t_1)\left\langle\begin{bmatrix} [\psi_\uparrow(1),\psi_\uparrow^\dagger(2)]_+ & [\psi_\uparrow(1),\psi_\downarrow(2)]_+ \\ -[\psi_\downarrow^\dagger(1),\psi_\uparrow^\dagger(2)]_+ & -[\psi_\downarrow^\dagger(1),\psi_\downarrow(2)]_+ \end{bmatrix}\right\rangle, \tag{2.3}$$

$$G^K=G^K(1,2)=-i\left\langle\begin{bmatrix} [\psi_\uparrow(1),\psi_\uparrow^\dagger(2)]_- & [\psi_\uparrow(1),\psi_\downarrow(2)]_- \\ -[\psi_\downarrow^\dagger(1),\psi_\uparrow^\dagger(2)]_- & -[\psi_\downarrow^\dagger(1),\psi_\downarrow(2)]_- \end{bmatrix}\right\rangle. \tag{2.4}$$

In Eqs. (2.2)–(2.4) $\psi(1)$ and $\psi^\dagger(1)$ denote the electron field operators $\psi(\vec{r}_1,t_1)$ and $\psi^\dagger(\vec{r}_1,t_1)$. In the following we use units such that $\hbar=k_B=c=1$.

The matrix Green function (2.1) satisfies the Dyson equation

$$(\hat{G}_0^{-1}-\hat{\Sigma})\otimes\hat{G}=\delta(1-2)\,, \tag{2.5}$$

where $\otimes$ implies integration over internal variables $(A\otimes B)(1,2)=\int d3\,A(1,3)B(3,2)$. The operator $\hat{G}_0^{-1}$ is the inverse of the noninteracting Green function. A convenient equation for $\hat{G}$, more closely related to a kinetic equation, is obtained by subtracting the conjugate of Eq. (2.5) from Eq. (2.5) itself:

$$(\hat{G}_0^{-1}-\hat{\Sigma})\otimes\hat{G}-\hat{G}\otimes(\hat{G}_0^{-1}-\hat{\Sigma})=0\,. \tag{2.6}$$

The Green function is a function of two sets of spatial coordinates, but it is more convenient to transform to the center-of-mass and relative coordinates and then perform a Fourier transformation, so that the Green function depends on the center-of-mass coordinate $\vec{R}$ and the momentum variable $\vec{p}$,

$$\hat{G}(\vec{R},\vec{p},t_1,t_2)=\int d\vec{r}\,e^{-i\vec{p}\cdot\vec{r}}\hat{G}(\vec{R}+\tfrac{1}{2}\vec{r},\vec{R}-\tfrac{1}{2}\vec{r},t_1,t_2)\,. \tag{2.7}$$

The reason for doing this transformation is that the Green function is a rapidly varying function of the relative coordinate (length scale p_F^{-1}, where p_F is the Fermi momentum), but a slowly varying function of the center-of-mass coordinate with a length scale characterized by the wave vector of the external perturbation. The wave vector and frequency of the external perturbation is assumed to be small compared with the Fermi wave vector and the chemical potential, respectively. This allows us to simplify the Dyson equation (2.6) because we can make the following approximation:

$$\begin{aligned}\int d\vec{r}_3dt_3\hat{\Sigma}(\vec{r}_1t_1,\vec{r}_3t_3)\hat{G}(\vec{r}_3t_3,\vec{r}_2t_2)&\\ \simeq\int dt_3\hat{\Sigma}(\vec{R},\vec{p};t_1,t_3)\hat{G}(\vec{R},\vec{p};t_3,t_2)&\\ \equiv[\hat{\Sigma}(\vec{R},\vec{p})\circ\hat{G}(\vec{R},\vec{p})](t_1,t_2)\,,&\end{aligned} \tag{2.8}$$

which defines the associative dot product $\circ$. The inverse of the nonvanishing Green function G_0^{-1} is within the same approximation given by

$$\begin{aligned}\hat{G}_0^{-1}=\{\,&i\hat{\tau}_3\partial_{t_1}-\xi(p)+i\vec{v}_F\cdot[\tfrac{1}{2}\vec{\nabla}_{\vec{R}}-ie\vec{A}(\vec{R},t_1)\hat{\tau}_3]\\ &-e\phi(\vec{R},t_1)\}\delta(t_1-t_2)\,,\end{aligned} \tag{2.9}$$

where τ_3 is the third Pauli matrix, $\xi(p)=p^2/2m-\mu$ is the normal-state quasiparticle energy measured with respect to the chemical potential μ, and $\vec{v}_F$ is the Fermi velocity. The vector potential is denoted by $\vec{A}$ and ϕ is the scalar potential. The approximation defined by Eqs. (2.8) and (2.9) is called the quasiclassical approximation. As written, (2.9) applies to a free-electron model with m being the electron mass and $\vec{v}_F=\vec{p}_F/m$. We may, with no loss of generality, replace m by an effective mass m^*, thus taking into account some of the effects of the electronic band structure. The key assumption, however, in using (2.9) for a real metal is that the effects of band anisotropy may be neglected.

In the following we only consider time-independent external perturbations in situations where the vector potential $\vec{A}$ may be set equal to zero. If we perform a Fourier transformation with respect to the relative time $t=t_1-t_2$, the dot product then reduces to an ordinary product. If we adopt the convention

$$[i\vec{v}_F\cdot\vec{\nabla}_{\vec{R}},G]_-=i\vec{v}_F\cdot\vec{\nabla}_{\vec{R}}G(\vec{R},\vec{p},E)\,, \tag{2.10}$$

then we may, within the quasiclassical approximation, write the Dyson equation as

$$[\hat{H},\hat{G}]_-=0\,, \tag{2.11}$$

where

$$\hat{H}=[E\tau_3+i\vec{v}_F\cdot\vec{\nabla}_{\vec{R}}-e\phi(\vec{R})]-\hat{\Sigma}(\vec{R},\vec{p},E)=\hat{g}_0^{-1}-\hat{\Sigma}\,. \tag{2.12}$$

A consequence of the quasiclassical approximation is that the only momentum-dependent terms in (2.11) are the self-energy and the Green function. In the following we

assume that the self-energy depends only on the direction of the momentum $\hat{p}=\vec{p}/|\vec{p}|$, with its magnitude fixed at the Fermi momentum p_F. This allows us to integrate the Green function in Eq. (2.11) over the magnitude of the momentum, corresponding to the variable $\xi(p)$ $(=p^2/2m-\mu)$, and to introduce the quasiclassical Green function

$$\hat{g}(\vec{R},\hat{p},E)=\frac{i}{\pi}\int d\xi\,\hat{G}(\vec{R},\vec{p},E)\ . \tag{2.13}$$

The equation of motion for the quasiclassical Green function (2.13) is found by integrating (2.11),

$$[\hat{H},\hat{g}]_-=0\ . \tag{2.14}$$

This equation must be supplemented by the normalization condition[6,8]

$$\hat{g}\hat{g}=1\ , \tag{2.15}$$

because (2.14) is homogeneous and hence does not determine $\hat{g}$ uniquely. Equations (2.14) and (2.15) are the fundamental equations in the derivation of a general kinetic equation for superconductors. The diagonal part of the equation of motion (2.14) determines the retarded and advanced functions, while the off-diagonal part becomes an equation for the distribution function which is associated with g^K.

A. The distribution functions

In equilibrium we may use the identity

$$\langle\psi^\dagger(\vec{r}_1,t_1)\psi(\vec{r}_2,t_2)\rangle=\langle\psi(\vec{r}_2,t_2)\psi^\dagger(\vec{r}_1,t_1+i/T)\rangle\ , \tag{2.16}$$

where T is the temperature, and the definitions (2.2)—(2.4), to show that

$$g^K(E)=[g^R(E)-g^A(E)][1-2f^0(E)]\ . \tag{2.17}$$

Here $f^0(E)=(e^{E/T}+1)^{-1}$ is the Fermi-distribution function. In the nonequilibrium case, g^K contains contributions from the retarded and advanced functions as well as the distribution functions, and the representations of g^K discussed below are an attempt to separate the two contributions.

The normalization condition (2.15) is, in a more detailed form,

$$g^Rg^R=1=g^Ag^A\ , \tag{2.18}$$

$$g^Rg^K+g^Kg^A=0\ . \tag{2.19}$$

A particular solution to Eq. (2.19) is

$$g^K=g^Rh-hg^A\ , \tag{2.20}$$

where h is an arbitrary distribution matrix. The particular choice of distribution functions introduced by Schmid and Schön[9] corresponds to introducing a diagonal distribution matrix and the scalar distribution functions f^L and f^T,

$$h=(1-2f^L)-2f^T\tau_3\ . \tag{2.21}$$

As we shall show below, (2.20) and (2.21) do not succeed completely in separating the density of states and the quasiparticle distribution function. An alternative way to make the separation is described by Shelankov,[13] who introduced the following solution to (2.19):

$$g^K=\tfrac{1}{2}(P_1^RF_1P_1^A+P_2^RF_2P_2^A)\ , \tag{2.22}$$

where F_1 and F_2 are arbitrary distribution matrices and $P_{1(2)}^R$ and $P_{1(2)}^A$ are defined by

$$\left.\begin{matrix}P_1^R\\P_2^R\end{matrix}\right\}=1\pm g^R\ , \tag{2.23}$$

$$\left.\begin{matrix}P_1^A\\P_2^A\end{matrix}\right\}=1\mp g^A\ . \tag{2.24}$$

$P_i^{R\,(A)}$ has the property of a projection operator, since it follows from the normalization condition (2.18) and the definitions (2.23) and (2.24) that

$$\begin{aligned}&P_i^{R\,(A)}P_i^{R\,(A)}=2P_i^{R\,(A)}\ ,\\&P_1^{R\,(A)}P_2^{R\,(A)}=0=P_2^{R\,(A)}P_1^{R\,(A)}\ .\end{aligned} \tag{2.25}$$

We assume that F_1 and F_2 are proportional to the unit matrix. The symmetry properties of g^K, when states with opposite spins are equally populated, allow us to introduce the real distribution function f, defined by

$$F_1(\vec{R},\hat{p},E)=1-2f(\vec{R},\hat{p},E)\ , \tag{2.26}$$

$$F_2(\vec{R},\hat{p},E)=1-2f(\vec{R},-\hat{p},-E)\ , \tag{2.27}$$

which, in the clean, weak-coupling limit reduces to the usual quasiparticle distribution function within a semiconductor model. As long as we neglect spatial gradients of the spectral densities, we may expand g^R and g^A on the Pauli matrices τ_1 and τ_3:

$$g^R=\alpha\tau_3+\beta\tau_1\ , \tag{2.28}$$

$$g^A=-\alpha^*\tau_3+\beta^*\tau_1\ , \tag{2.29}$$

where an asterisk denotes complex conjugation. The generalized densities of states are now defined as

$$\alpha=N_1+iR_1\ , \tag{2.30}$$

$$\beta=N_2+iR_2\ , \tag{2.31}$$

where N_i and R_i are, respectively, even and odd functions under the transformation $(\hat{p},E)\rightarrow(-\hat{p},-E)$.

The connection between the distribution functions introduced by Eq. (2.21) and the ones introduced by Eqs. (2.26) and (2.27) is

$$1-2f^L(\hat{p},E)=f(-\hat{p},-E)-f(\hat{p},E) \tag{2.32}$$

and

$$f^T(\hat{p},E)=\tfrac{1}{2}\frac{(N_1^2-R_2^2)(\hat{p},E)}{N_1(\hat{p},E)}\times[f(\hat{p},E)+f(-\hat{p},-E)-1]\ . \tag{2.33}$$

The relation between f^T and the conventional distribution

function for Bogoliubov quasiparticles has been discussed in Ref. 16.

B. Self-energy and self-consistency equations

The self-energy entering the equation of motion (2.14) consists of contributions from the phonons, nonmagnetic and magnetic impurities. In the following, we discuss each of the contributions separately and then derive the self-consistency equations valid for strong- as well as weak-coupling superconductors.

The self-energy from nonmagnetic impurities is

$$\hat{\Sigma}_i(\hat{p},E)=-\frac{i}{2}\frac{1}{\tau_{\rm imp}}\int\frac{d\Omega_{\hat{p}'}}{4\pi}w(\hat{p}\cdot\hat{p}')\hat{g}(\hat{p}',E)$$
$$=-\frac{i}{2}\frac{1}{\tau_{\rm imp}}\langle\hat{g}\rangle_i\ , \tag{2.34}$$

where $1/\tau_{\rm imp}$ is the s-wave scattering rate and $w(\hat{p}\cdot\hat{p}')$ is the normalized scattering probability which is equal to unity for s-wave scattering. The self-energy from magnetic impurities is

$$\hat{\Sigma}_s(\hat{p},E)=-\frac{i}{2}\frac{1}{\tau_s}\int\frac{d\Omega_{\hat{p}'}}{4\pi}w_s(\hat{p}\cdot\hat{p}')\hat{\tau}_3\hat{g}(\hat{p}',E)\hat{\tau}_3$$
$$=-\frac{i}{2}\frac{1}{\tau_s}\hat{\tau}_3\langle\hat{g}\rangle_s\hat{\tau}_3\ , \tag{2.35}$$

where τ_s^{-1} is the s-wave spin-flip scattering rate and $w_s(\hat{p}\cdot\hat{p}')$ is the normalized scattering probability. The phonon self-energy is within the Migdal approximation

$$\Sigma_{\rm ph}^{R\,(A)}(\hat{p},E)=\frac{N(0)}{4}\int dE'\frac{d\Omega_{\hat{p}'}}{4\pi}[g^{R\,(A)}(\hat{p}',E')D^K(\hat{p}'-\hat{p},E'-E)+g^K(\hat{p}',E')D^{A\,(R)}(\hat{p}'-\hat{p},E'-E)]\ , \tag{2.36}$$

where $N(0)$ is the density of states at the Fermi surface for a single spin in the normal metal, and

$$\Sigma_{\rm ph}^K(\hat{p},E)=\frac{N(0)}{4}\int dE'\frac{d\Omega_{\hat{p}'}}{4\pi}[\,g^K(\hat{p}',E')D^K(\hat{p}'-\hat{p},E'-E)-(g^R-g^A)(\hat{p}',E')(D^R-D^A)(\hat{p}'-\hat{p},E'-E)]\ , \tag{2.37}$$

with the phonons assumed to be in equilibrium. We use the following spectral representation for the phonon Green functions:

$$\left.\begin{matrix}D^R(\vec{q},\omega)\\D^A(\vec{q},\omega)\end{matrix}\right\}=\sum_\mu|g_{\vec{q}}^\mu|^2\int d\Omega\frac{\rho_\mu(\vec{q},\Omega)}{\omega-\Omega\pm i\delta}\ , \tag{2.38}$$

$$D^K(\vec{q},\omega)=(D^R-D^A)[1+2N(\omega)]\ , \tag{2.39}$$

where ρ_μ is the spectral densities, g_q^μ is the electron-phonon coupling constant for phonons of polarization μ, and $N(\omega)$ is the Bose function.

In the following, we expand the self-energies $\Sigma^{R\,(A)}$ on the Pauli matrices by the ansatz

$$\Sigma^R=(1-Z)E\tau_3-i\Phi_1\tau_1\ ,$$
$$\Sigma^A=(1-Z^*)E\tau_3-i\Phi_1^*\tau_1\ , \tag{2.40}$$

where we assume that the 1 component is zero. We are only considering kinetic equations linear in the deviation from equilibrium, and as we shall see in the next sections, we only need the equilibrium part of the self-consistency equations for the parameters in (2.40). The distribution matrices F_1 and F_2 are assumed to be proportional to the unit matrix, and the distribution function f defined by (2.26) and (2.27) is used.

When the generalized densities of states are independent of $\hat{p}'$, we can introduce the effective phonon density of states $\alpha^2_{\vec{p}}F$ by the definition

$$\alpha^2_{\vec{p}}F(E)=N(0)\sum_\mu\int\frac{d\Omega_{\hat{p}'}}{4\pi}|g^\mu_{\vec{p}',-\vec{p}}|^2\rho_\mu(\vec{p}'-\vec{p},E)\ . \tag{2.41}$$

For isotropic or dirty systems, with s-wave scattering from impurities, the self-consistency equations are averaged over all directions to obtain the well-known Eliashberg equations:

$$(1-Z)E=-\frac{1}{2\pi}\int dx\,N_1(x)\int dy\frac{B(x,x-y)}{x-y-E-i\delta}$$
$$-\frac{i}{2}\left[\frac{1}{\tau_{\rm imp}}+\frac{1}{\tau_s}\right][N_1(E)+iR_1(E)]\ , \tag{2.42}$$

$$\Phi_1(E)=\frac{1}{2\pi}\int dx\,R_2(x)\int dy\frac{B(x,x-y)}{x-y-E-i\delta}$$
$$+\frac{i}{2}\left[\frac{1}{\tau_{\rm imp}}-\frac{1}{\tau_s}\right][N_2(E)+iR_2(E)]\ , \tag{2.43}$$

where $B(E,E')$ is

$$B(E,E')=\pi\alpha^2F(|E-E'|)\times\frac{\cosh(E'/2T)}{\sinh(|E-E'|/2T)\cosh(E/2T)}\ , \tag{2.44}$$

and α^2F is the angular average of $\alpha^2_{\vec{p}}F$.

We may reach the weak-coupling limit of the self-consistency equations, where retardation effects are neglected, by taking the limit of infinite sound velocity. The phonon Green functions (2.38) and (2.39) are then

$$D^{R\,(A)}(\vec{q},\omega)=-\frac{\lambda(\vec{q})}{N(0)},\quad D^K(\vec{q},\omega)=0\ , \tag{2.45}$$

where

$$\lambda(\vec{q})=2N(0)\sum_\mu\frac{|g^\mu_{\vec{q}}|^2}{\omega^\mu_{\vec{q}}}\ . \tag{2.46}$$

If $\lambda(\vec{q})$ is constant, $\lambda(\vec{q})=\lambda$, the phonon self-energy (2.36) then reduces to

$$\Sigma^R=-\frac{\lambda}{4}\int dE'\frac{d\Omega_{\hat{p}'}}{4\pi}g^K(\hat{p}',E') . \tag{2.47}$$

The self-consistency equation for the gap Δ is obtained from off-diagonal (od) terms of Σ^R, since

$$(\Sigma^R)^{\rm od}=-i\Delta\tau_1 . \tag{2.48}$$

When we take the limit of infinite sound velocity, we lose the effects of renormalization, scattering, and pair breaking by the phonons. To retain the scattering and pair-breaking processes, we have to keep the imaginary part of $\mathcal{Z}E$. The phonon contribution to $\mathrm{Im}(\mathcal{Z}E)$ is obtained from (2.42) as

$$\mathrm{Im}(\mathcal{Z}E)=\frac{1}{2\tau(E)}=\tfrac{1}{2}\int dx\, N_1(x)B(x,E) . \tag{2.49}$$

C. Densities of states

In this section we discuss the equations for the spectral densities, which determine how pair-breaking processes affect the generalized densities of states. As we shall see later in specific examples, the smearing of the densities of states depends on the particular mechanism considered. While an arbitrary small rate of electron-phonon scattering always makes a superconductor gapless in the sense that $N_1(E)$ differs from zero for all energies E, it takes a finite spin-flip scattering rate to make it gapless. The nonmagnetic impurities cause pair breaking whenever the spectral densities depend on the direction in momentum space, a situation which we neglect in the following, where we only consider isotropic systems.

Equations for the spectral densities α and β are obtained from the diagonal part of the equation of motion (2.14) and the normalization condition (2.18). Due to the connection (2.28) and (2.29) between g^R and g^A, we only have to consider the equation of motion for g^R:

$$[H^R,g^R]_-=0 , \tag{2.50}$$

which provides us with four equations. The diagonal part of the normalization condition $g^Rg^R=1$ yields the additional equation

$$\alpha^2+\beta^2=1 . \tag{2.51}$$

We need only two equations to determine the spectral densities and shall only consider one of the off-diagonal components of (2.50), together with (2.51). The off-diagonal part of (2.50) gives

$$\mathcal{Z}E\beta-i\alpha\Phi_1+\frac{i}{\tau_s}\alpha\beta=0 , \tag{2.52}$$

which together with (2.51) results in a quartic equation for α,

$$\Gamma_s^2\alpha^4-2i\Gamma_s\mathcal{Z}E\alpha^3+[\Phi_1^2-(\mathcal{Z}E)^2-\Gamma_s^2]\alpha^2 +2i\Gamma_s\mathcal{Z}E\alpha+(\mathcal{Z}E)^2=0 , \tag{2.53}$$

where Γ_s is the spin-flip scattering rate. When both scattering mechanisms are present (2.53) has to be solved numerically, while the generalized densities of states in the absence of magnetic impurities are

$$N_1+iR_1=\frac{\mathcal{Z}E}{[(\mathcal{Z}E)^2-\Phi_1^2]^{1/2}}=\frac{E}{(E^2-\Delta^2)^{1/2}} , \tag{2.54}$$

$$N_2+iR_2=\frac{i\Phi_1}{[(\mathcal{Z}E)^2-\Phi_1^2]^{1/2}}=\frac{i\Delta}{(E^2-\Delta^2)^{1/2}} , \tag{2.55}$$

where $\mathcal{Z}$ and ϕ have to be determined from the Eliashberg equations (2.42) and (2.43). The complex gap function Δ is defined as $\Delta=\Phi_1/\mathcal{Z}$.

D. The kinetic equation

The kinetic equation is obtained from the off-diagonal part of the equation of motion (2.14), which takes the form

$$H^Rg^K-g^KH^A+g^R\Sigma^K-\Sigma^Kg^A=0 . \tag{2.56}$$

Using the representation (2.22) of g^K and the orthogonality (2.25) of the operators defined in (2.23), (2.24) together with their equation of motion, we find the following equation for F_1:

$$\mathrm{tr}(P_1^AP_1^R)i\vec{v}_F\cdot\vec{\nabla}F_1=\mathrm{tr}\{P_1^AP_1^R[(\Sigma^R-\Sigma^A)F_1-\Sigma^K]\} , \tag{2.57}$$

where we have identified a driving term by the left-hand side and put the remaining collision terms on the right-hand side. The collision terms consist of contributions from the phonons, nonmagnetic and magnetic impurities. In the Appendix we express the collision integrals for each scattering mechanism separately, in terms of the distribution function f defined by (2.26) and (2.27), and since we are only interested in small deviations from equilibrium, we linearize in the deviation from local equilibrium $\delta f=f-f^0$. The kinetic equation is then

$$(N_1^2-R_2^2)\vec{v}_F\cdot\vec{\nabla}f=(I_{\rm ph}+I_{\rm imp}+I_s)(\delta f) . \tag{2.58}$$

E. The thermal current and the charge density

The heat-current operator may be found by considering the energy-momentum tensor for the coupled electron-phonon system.[21] The energy-current operator is then of the form $\hat{\vec{u}}=\hat{\vec{u}}_e+\hat{\vec{u}}_{\rm ph}$. In the following we assume that the phonons are in equilibrium—that is, we can neglect the energy current $\vec{u}_{\rm ph}$ from the phonons. The heat-current operator is then

$$\hat{\vec{J}}_{\rm th}=\hat{\vec{u}}_e-\mu\hat{\vec{J}} , \tag{2.59}$$

where μ is the chemical potential and $\hat{\vec{J}}$ is the particle current operator. Measuring energy from the chemical potential, the electronic heat-current operator is[4]

$$\hat{\vec{J}}_{\rm th}=-\frac{1}{2m}\sum_\sigma(\partial_{t_1}\vec{\nabla}_2+\partial_{t_2}\vec{\nabla}_1)\psi_\sigma^\dagger(2)\psi_\sigma(1)\,|_{2\to1} . \tag{2.60}$$

Using the definitions of $G^{K,R,A}$, we find the heat current to be

$$\vec{J}_{\rm th}=-\frac{N(0)p_F}{4m}\int dE\frac{d\Omega_{\hat{p}}}{4\pi}E\hat{p}\,{\rm tr}g^K\,, \tag{2.61}$$

which in the static case may be rewritten as

$$\vec{J}_{\rm th}=-\frac{N(0)p_F}{m}\int dE\frac{d\Omega_{\hat{p}}}{4\pi}E\hat{p}(N_1^2-R_2^2)[2f(\hat{p},E)-1]\,. \tag{2.62}$$

Finally, we consider the charge density

$$\rho(1)=e\sum_\sigma\langle\psi_\sigma^\dagger(1)\psi_\sigma(1)\rangle\,, \tag{2.63}$$

which may be expressed in terms of g^K,

$$\rho=-\frac{eN(0)}{4}\int dE\frac{d\Omega_{\hat{p}}}{4\pi}{\rm tr}[g^K-\tau_3(g^R-g^A)]\,. \tag{2.64}$$

Since the charge density is a gauge invariant quantity (2.64) must have the form

$$\rho=-eN(0)\left[2e\phi+\tfrac{1}{4}\int dE\frac{d\Omega_{\hat{p}}}{4\pi}{\rm tr}[g^K-\tau_3(g^R-g^A)]\right], \tag{2.65}$$

where ϕ is the scalar potential introduced in (2.9). In the static case we have

$$\rho=-2eN(0)\left[e\phi-\tfrac{1}{2}\int dE\frac{d\Omega_{\hat{p}}}{4\pi}\times\{(N_1^2-R_2^2)[2f(\hat{p},E)-1]+N_1\}\right]. \tag{2.66}$$

In using this expression for the charge-density one should remember that the quasiclassical Green functions only represent correctly those contributions to the density which come from regions near the Fermi surface. The contributions from regions far from the Fermi surface are represented by the scalar potential ϕ.

III. THERMAL CONDUCTIVITY

The collision integrals are most conveniently discussed in terms of the usual deviation function ψ, which for thermal conductivity is defined by $f=f^0+f^0(1-f^0)\hat{p}\cdot\vec{\nabla}T\psi$, where f^0 is the Fermi function and $\vec{\nabla}T$ is the temperature gradient. We then eliminate the common factor $\hat{p}\cdot\vec{\nabla}T$ in Eq. (2.58) and average over all directions. The contributions to the collision integrals are then the following.

(1) Phonons: From the Appendix we find

$$I_{\rm ph}(\psi)=\frac{-1}{4\cosh^2(E/2T)}\int_{-\infty}^{\infty}dE'\left[B(E',E)[N_1(E)N_1(E')-R_2(E)R_2(E')]\psi(E)\right.$$
$$\left.-B_1(E',E)[N_1^2(E)-R_2^2(E)][N_1^2(E')-R_2^2(E')]\left[1+\frac{N_2(E)N_2(E')}{N_1(E)N_1(E')}\right]\psi(E')\right], \tag{3.1}$$

where B is defined by (2.24) and B_1 by an identical expression except that α^2F in (2.44) is replaced by α_1^2F, an effective density of states for transport which is evaluated in the same way as α^2F, but with the inclusion of an additional factor $\hat{p}\cdot\hat{p}'$ in the sum over phonon states. Here $\hat{p}$ and $\hat{p}'$ are the directions of the initial and final electrons in the process in which an electron is scattered by a phonon.

(2) Impurities: From the Appendix we find

$$I_{\rm imp}(\psi)=-\frac{N_1^2(E)-R_2^2(E)}{\tau_{\rm imp}^{\rm tr}}\frac{\psi(E)}{4\cosh^2(E/2T)}\,, \tag{3.2}$$

where $\tau_{\rm imp}^{\rm tr}$ is the transport scattering time, given by the usual weighted average of the collision probability $w(\hat{p}\cdot\hat{p}')$,

$$\frac{1}{\tau_{\rm imp}^{\rm tr}}=\frac{1}{\tau_{\rm imp}}\int_{-1}^{1}dx[\tfrac{1}{2}w(x)(1-x)]\,. \tag{3.3}$$

In the following we assume that the magnetic impurities only have a s-wave component, so the contribution is

$$I_s(\psi)=-\frac{N_1^2(E)+R_2^2(E)}{\tau_s}\frac{\psi(E)}{4\cosh^2(E/2T)}\,. \tag{3.4}$$

The full kinetic equation is, according to (2.58), (3.1), (3.2), and (3.4),

$$(N_1^2-R_2^2)\frac{v_FE}{T^2}=-\left[\int_{-\infty}^{\infty}dE'\,B(E',E)(N_1N_1'-R_2R_2')+\frac{N_1^2-R_2^2}{\tau_{\rm imp}^{\rm tr}}+\frac{N_1^2+R_2^2}{\tau_s}\right]\psi(E)$$
$$+\int_{-\infty}^{\infty}dE'\,B_1(E',E)(N_1^2-R_2^2)(N_1'^2-R_2'^2)\left[1+\frac{N_2N_2'}{N_1N_1'}\right]\psi(E')\,. \tag{3.5}$$

The electronic heat conductivity κ is defined by

$$\vec{J}_{\rm th}=-\kappa\vec{\nabla}T\ , \tag{3.6}$$

where $\vec{J}_{\rm th}$ is given by Eq. (2.62). In terms of ψ we have

$$\kappa=\frac{N(0)v_F}{3}\int_0^\infty dE(N_1^2-R_2^2)\frac{E\psi(E)}{\cosh^2(E/2T)}\ . \tag{3.7}$$

We close this section by introducing the important parameter $\tau_{\rm in}$ characterizing the strength of the inelastic electron-phonon interaction. It is defined as the normal-state inelastic relaxation time at T_c and at the Fermi energy

$$\frac{1}{\tau_{\rm in}}=\left.\frac{2\,{\rm Im}(ZE)}{{\rm Re}Z}\right|_{T=T_c,\ E=0}$$
$$=\frac{4\pi}{{\rm Re}Z(0)}\int_0^\infty dE\frac{\alpha^2F(E)}{\sinh(E/T_c)}\ . \tag{3.8}$$

In the weak-coupling limit we use a Debye model, where $\alpha^2F=bE^2$. Here b is of the order of the inverse Debye temperature Θ_D squared. For this model one obtains

$$\frac{1}{\tau_{\rm in}}=\frac{14\pi\zeta(3)T_c^3b}{{\rm Re}Z(0)}\ . \tag{3.9}$$

Furthermore, if $\alpha^2F=0$ for $E>\Theta_D$, one has ${\rm Re}Z(0)=1+\lambda$, where $\lambda=b\Theta_D^2$. In the case of the strong-coupling superconductor Pb, we use the model for α^2F discussed in Ref. 22 (case 2, p. 532), but we include a Debye tail for frequencies below the transverse peak which we estimate from Ref. 23 to be

$$\alpha^2F(E)=2.75\times10^{-3}E^2\ , \tag{3.10}$$

where E is measured in meV. The Debye tail (3.10) is particularly important at low temperatures. In this strong-coupling case we obtain

$$\frac{{\rm Re}Z(0)}{\tau_{\rm in}T_c}=0.15\ . \tag{3.11}$$

A. Weak-coupling limit with nonmagnetic impurities

We now proceed to determine the electronic thermal conductivity in the weak-coupling limit from solutions to the kinetic equation (3.5). We assume that the phonon spectrum is described by the Debye model discussed above (3.9). In the low-temperature regime $T/\Theta_D\ll1$ in which we are interested, the momentum of the scattering phonons may be neglected compared with the Fermi momentum. That is, we can take $B_1=B$ in the collision integral, which is correct to order $(T/\Theta_D)^2$.

A consequence of the Debye model is that the normal-state electronic thermal conductivity for a pure sample at temperatures much lower than the Debye temperature is proportional to T^{-2}, due to the freezing out of the number of phonons.

In the quasiparticle limit, where we neglect the influence of pair breaking on the generalized densities of states, we have

$$N_1=\frac{|E|}{(E^2-\Delta^2)^{1/2}}\Theta(|E|-\Delta)\ , \tag{3.12}$$

$$R_1=-\frac{E}{(\Delta^2-E^2)^{1/2}}\Theta(\Delta-|E|)\ , \tag{3.13}$$

and

$$N_2=\frac{\Delta}{(\Delta^2-E^2)^{1/2}}\Theta(\Delta-|E|)\ , \tag{3.14}$$

$$R_2=\frac{\Delta}{(E^2-\Delta^2)^{1/2}}{\rm sgn}(E)\Theta(|E|-\Delta)\ . \tag{3.15}$$

The clean limit of the kinetic equation (3.5) then reduces to that derived by Bardeen *et al.*[1] and solved numerically by Tewordt,[24] who found the limiting slope of $\kappa_s(T)/\kappa_N(T)$, as $t=T/T_c$ approaches 1 from below, to be 1.62. In our calculation we find the limiting slope to be 1.8. The difference is probably caused by the high resolution we use during the numerical inversion of the collision operator. The influence of impurities is conveniently discussed in terms of the parameter

$$c=\frac{\tau_{\rm in}}{[{\rm Re}Z(0)]\tau_{\rm imp}^{\rm tr}}\ . \tag{3.16}$$

In Fig. 1 we plot $\kappa_s(T)/\kappa_N(T)$ as a function of T/T_c for a clean and a dirty superconductor. In the clean limit, where $c=0$, the overall feature is the same as that found by Tewordt[24] except for the larger slope close to T_c. Note that the dirty-limit result has zero slope as $t\to1$ since $[\kappa_N(T)-\kappa_s(T)]/\kappa_N(T)$ is proportional to Δ^3 when the temperature is near T_c.

To obtain a better understanding of what is happening we plot in Fig. 2 $\kappa_s(T)/\kappa_N(T_c)$, the thermal conductivity normalized to its value at T_c, for a number of different impurity concentrations. We see that even though the density of quasiparticles is decreasing below T_c, the clean limit result is still increasing as the temperature is lowered, due to the decrease of the number of phonons. However, for $T\simeq0.3T_c$ it reaches a maximum and then falls off very rapidly due to the exponential decrease of

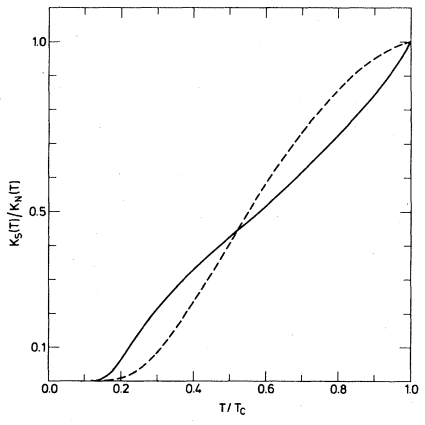

FIG. 1. Temperature dependence of the electronic thermal conductivity κ_s for a pure and a dirty (dashed curve) weak-coupling superconductor, normalized to the normal-state value at the same temperature.

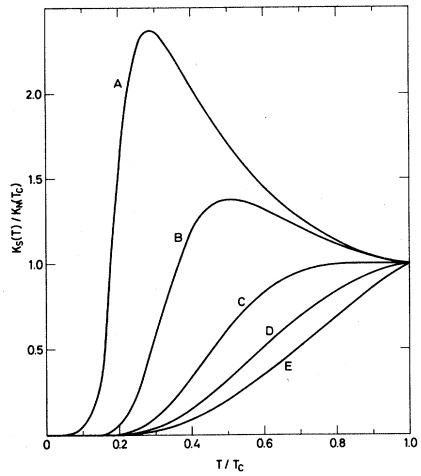

FIG. 2. Temperature dependence of the electronic thermal conductivity κ_s for a weak-coupling superconductor, normalized to the value at T_c, for various impurity concentrations, corresponding to different values of the parameter c defined in (3.16). *A*, $c=0$; *B*, $c=0.1$; *C*, $c=1.0$; *D*, $c=5.0$; *E*, $c=\infty$.

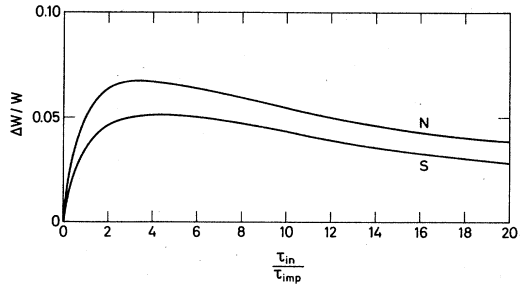

FIG. 3. Deviation from Matthiessen's rule $\Delta W/W$ for a weak-coupling superconductor in the superconducting (s) as well as normal state (N) as a function of $\tau_{\text{in}}/\tau_{\text{imp}}$, at the temperature $T=0.96T_c$.

the number of quasiparticles at low temperatures. When impurities are added, the maximum shifts to higher temperatures and eventually disappears when $c\simeq 1$. If $c\gtrsim 1$, then $\kappa_s(T)/\kappa_N(T_c)$ always decreases with temperature. The characteristic low-temperature behavior of κ_s for a clean superconductor may be found directly from the kinetic equation and the expression for the heat current. The result is that

$$\kappa_s(T)\propto(\Delta/T)^4 e^{-\Delta/T}\ \text{for}\ T/\Delta\ll 1\ . \tag{3.17}$$

If we define τ_κ by the kinetic expression $\kappa_s=\frac{1}{3}c_v\langle v^2\rangle\tau_\kappa$, where $\langle v^2\rangle=(T/\Delta)v_F^2$ is the average of the group velocity squared, then we see from (3.17) that $\tau_\kappa^{-1}\propto T^{7/2}$, which is the same temperature dependence as the electron-phonon relaxation rate $\tau^{-1}(\Delta)$ at low temperatures, $T\ll\Delta$. Note, however, that it is not possible to determine the coefficient in front of (3.17) analytically, as this requires the solution of the full integral equation.

The electronic part of the thermal resistivity is in the presence of two different scattering mechanisms, not simply the sum of resistivities calculated for each scattering mechanism separately. The difference, usually referred to as deviations from Matthiessen's rule (DMR), may be sizable. In Fig. 3 we show the calculated DMR for a weak-coupling superconductor. The DMR is defined as

$$\frac{\Delta W}{W}=\frac{W-W_{\text{ph}}-W_{\text{imp}}}{W}\ , \tag{3.18}$$

where ΔW is the DMR, W the total resistivity, and W_{ph} and W_{imp} the resistivities when phonons and impurities, respectively, are the only scattering mechanisms. We plot the result for the superconducting as well as the normal state at the temperature $t=0.96$. The result is that DMR is less than 7% of the total resistivity for all impurity concentrations, all temperatures below T_c, and both states.

The DMR is zero if the solutions belonging to each collision operator, when considered separately, differ only by a constant factor. We therefore plot in Fig. 4 the deviation function ψ for a pure superconductor at $T=0.90T_c$. The DMR is then due to the difference of ψ in Fig. 4 from a linear function of E, which according to (3.5) is the deviation function when the only scattering mechanism is that due to ordinary impurities.

B. Strong-coupling superconductor with nonmagnetic impurities

In this section we discuss the electronic thermal conductivity in a strong-coupling superconductor, taking Pb as a typical example. We use the effective phonon density of states α^2F shown in Fig. 5, which is consistent with tunneling measurements on Pb.[25] The kinetic equation (3.5) contains the effective phonon density of states for transport α_1^2F. For lack of information about this quantity, we assume in the numerical calculations presented below that it may be replaced by α^2F as in the weak-coupling case discussed above.

The generalized densities of states are now obtained from (2.54) and (2.55), where the complex functions Z and Φ_1 are determined by the Eliashberg equations (2.42) and (2.43) with the Coulomb pseudopotential parameter (Ref. 22) μ^* given by $\mu^*=0.11$.

The thermal conductivity for lead with nonmagnetic impurities is shown in Fig. 6, where $\kappa_s(T)/\kappa_N(T)$ is plotted as a function of T/T_c for the impurity concentrations $c=0$, 0.73, and ∞, where c is defined by (3.16). In the clean limit near T_c (curve *A*) we find the slope of

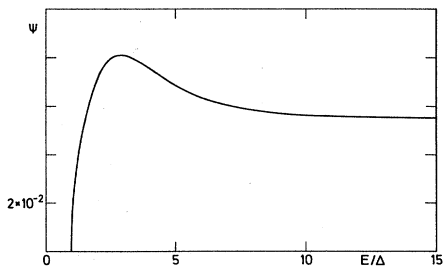

FIG. 4. Deviation function ψ as a function of energy for a weak-coupling superconductor at $T=0.90T_c$. The units of ψ are arbitrary.

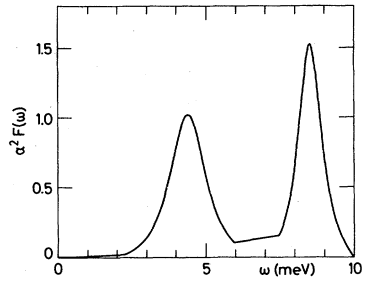

FIG. 5. Effective phonon density of states α^2F, used to model lead. The model is that discussed in Ref. 22 (case 2, p. 532) with the Debye tail given by (3.10) included.

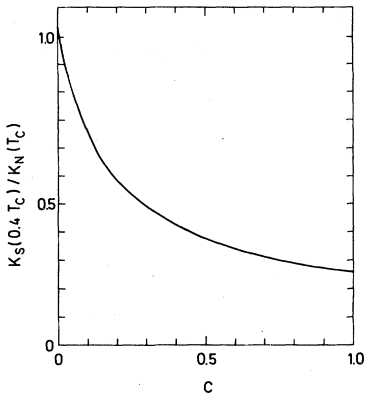

FIG. 8. Dependence of the electronic thermal conductivity κ_s on the impurity concentration c at $T=0.4T_c$. κ_s is normalized to the value at T_c.

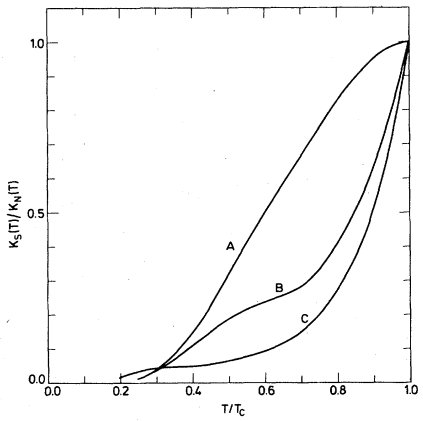

FIG. 6. Temperature dependence of the electronic thermal conductivity κ_s for lead, normalized to the normal-state value at the same temperature and for various impurity concentrations. *A*, $c=73$; *B*, $c=0.73$; *C*, $c=0$.

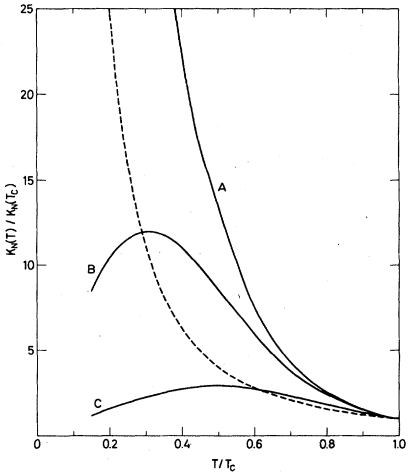

FIG. 9. Temperature dependence of the electronic thermal conductivity for lead in the normal state, normalized to the value at T_c, for various impurity concentrations. *A*, $c=0$; *B*, $c=0.073$; *C*, $c=0.73$. The dashed curve is the normal-state electronic thermal conductivity for a clean weak-coupling superconductor, with the temperature dependence $\kappa_N(T) \propto T^{-2}$.

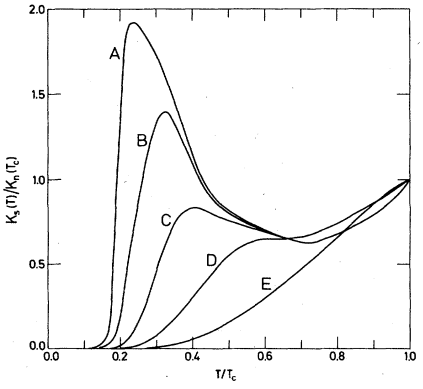

FIG. 7. Temperature dependence of the electronic thermal conductivity κ_s for lead, normalized to the value at T_c, for various impurity concentrations. *A*, $c=0$; *B*, $c=0.0073$; *C*, $c=0.073$; *D*, $c=0.73$; *E*, $c=73$.

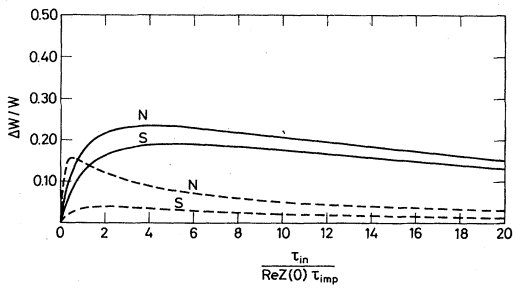

FIG. 10. Deviation from Matthiessen's rule $\Delta W/W$ for lead in the superconducting (S) as well as normal state (N) as a function of $\tau_{in}/\{[\mathrm{Re}Z(0)]\tau_{imp}\}$, for the temperatures $T=0.96T_c$ (solid curves) and $T=0.60T_c$ (dashed curves).

$\kappa_s(T)/\kappa_N(T)$ to be 7.2, which is in good agreement with experiment[2] but somewhat different from the approximate result of Ambegaokar and Woo[5] who found the slope to be 11.

To obtain a better understanding of this behavior, we plot in Fig. 7 $\kappa_s(T)/\kappa_N(T_c)$ for a number of impurity concentrations. The behavior of the clean-limit result (curve A) is very different from that of the weak-coupling clean limit result at temperatures greater than $T\simeq 0.3T_c$. The weak-coupling result is increasing when the temperature is lowered, while the curve for lead decreases. At lower temperatures, the curve for lead shows a minimum at $T\simeq 0.7T_c$ and then increases very rapidly. Below the maximum at $T\simeq 0.25T_c$, the thermal conductivity eventually drops to zero. The influence of impurities is also seen in Fig. 7, discussed in terms of the parameter c. It is seen that curves B and C follow the $c=0$ curve down to $T\simeq 0.6T_c$. The behavior for temperatures below $0.6T_c$ depends critically on the value of c, but the general behavior is that if $c\lesssim 1$ then κ_s has a maximum, while it always decreases if $c\gtrsim 1$.

In order to study the influence of the impurities in more detail, we also show in Fig. 8 the thermal conductivity of Pb at $T=0.4T_c$ as a function of c in the range $0<c<1$. In Fig. 9 we plot $\kappa_N(T)/\kappa_N(T_c)$ for three different values of c, together with the clean-limit result for a weak-coupling Debye model (dashed curve). The clean-limit result for lead (curve A) is increasing much faster than the weak-coupling limit result (dashed curve) for temperatures $T\gtrsim 0.4T_c$. At lower temperatures curve A essentially increases as T^{-2}. The influence of impurities on $\kappa_N(T)$ is shown in curves B and C for two different impurity concentrations.

In Fig. 10 we plot the deviation from Matthiessen's rule, defined by (3.18), for lead in the superconducting as well as the normal state and at the two temperatures $t=0.96$ and 0.60. At $t=0.96$, the DMR is large over a broad range of impurity concentrations in both states. The maximum DMR is, in the normal states, 24% of the total resistivity, while it is 19% in the superconducting state. At $t=0.60$, the normal-state DMR is peaked with a maximum of 16% for an impurity concentration $c\simeq 0.5$. The DMR in the superconducting state is below 4% for all impurity concentrations.

The explanation of the behavior of $\kappa_s(T)/\kappa_N(T_c)$ and the large deviations from Matthiessen's rule may be seen from the deviation function ψ, which we plot in Fig. 11 for pure lead at the temperature $t=0.90$. The main contribution to κ_s comes from excitations in the energy region $E/T\lesssim 6$; however, for Pb close to T_c the excitations with an energy $E/T\simeq 5-6$ are very effectively removed by recombination processes, where they recombine with a quasiparticle of energy $E\simeq\Delta$ to form a pair. This process has a large probability, due to the lowest peak in the effective phonon density of states α^2F. The removal of excitations is clearly seen in Fig. 11. The figure also shows how ψ is nonzero for energies below the gap, due to smearing of the densities of states. The effective removal of the "high-energy" excitations is the main reason for the drop in $\kappa_s(T)/\kappa_N(T_c)$ below T_c. Another reason is the larger ratio $2\Delta_{\rm Pb}(T=0)/T_c\simeq 4.3$, which means that the number

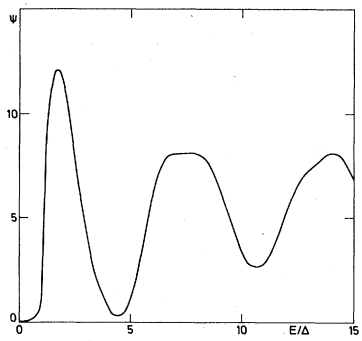

FIG. 11. Deviation function ψ for lead as a function of energy at the temperature $T=0.90T_c$. The units of ψ are arbitrary.

of excitations at a given temperature is less than in a weak-coupling superconductor, since the gap (at the gap edge) is known to follow[22]

$$\Delta_{\rm Pb}(T)=\Delta_{\rm Pb}(0)\frac{\Delta_{\rm BCS}(T)}{\Delta_{\rm BCS}(0)}\ . \tag{3.19}$$

At lower temperatures, the recombination processes of particles that contribute to the heat conductivity is not sufficient to reach the first peak in α^2F. This means that the dominating scattering channel loses weight, so the heat conductivity begins to rise. At even lower temperatures, it is only the Debye tail that determines the scattering, so $\kappa_s(T)$ should behave like a weak-coupling superconductor, which indeed is the case.

The behavior of the normal-state thermal conductivity $\kappa_N(T)/\kappa_N(T_c)$ is also explained in terms of the structure in the effective phonon density of states α^2F. We may use the same arguments as for the superconducting case discussed above if we replace recombination processes by scattering from a state above the Fermi surface to states below the Fermi surface.

The main numerical problem in calculating the electronic thermal conductivity of strong-coupling superconductors is to obtain the solutions to the Eliashberg equations, which enter the generalized densities of states. In Fig. 12, we have plotted the generalized density-of-state functions N_1 and N_2 for lead, obtained by solving the Eliashberg equations at temperature $T=0.96T_c$. They appear remarkably similar to those for the weak-coupling case in the absence of pair breaking, except for some broadening due to the finite quasiparticle lifetime. The most important difference is that the energy is measured in terms of the actual energy gap at the gap edge (3.19). This suggests that it is possible to obtain reasonable results by neglecting the broadening of the energy levels, that is, we use the density of states (3.12)—(3.15) with the gap following (3.19), and keep the model for the effective phonon density of states. Our numerical calculations show that this quasiparticle approximation is within 10% of the exact result for all temperatures and all impurity concentrations.

As discussed above, the low-temperature electronic thermal conductivity of pure lead is determined by the Debye tail of the effective phonon density of states. We

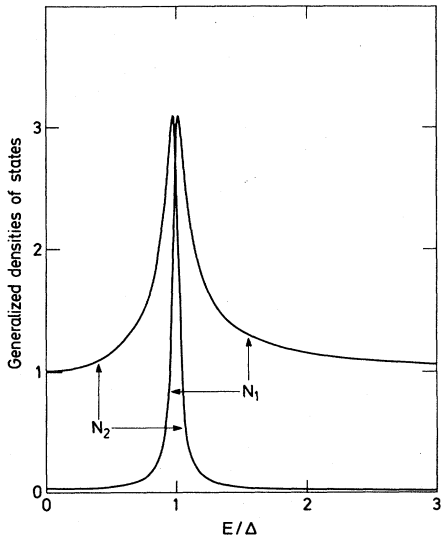

FIG. 12. Generalized densities of states N_1 and N_2 for lead for the case of scattering by phonons alone at the temperature $T=0.96T_c$. The gap at the gap edge is $\Delta_{Pb}(T=0.96T_c)=0.44$ meV.

can then use Eq. (3.17) as an approximate expression for the temperature dependence of κ_s for $T/\Delta \ll 1$, provided the value of the gap is taken to be the zero-temperature result appropriate for Pb.

C. Experiments on tin and lead

The thermal conductivity of tin and lead samples at low temperatures has been investigated by many authors, and a detailed summary with plots of the various experiments is given in Ref. 26. Here we consider the measurements performed by Guénault[3] on pure tin, and measurements on pure lead performed more recently by Mezahov-Deglin[18] and Odoni *et al.*[27] The experiments on tin[3] give a slope of $\kappa_s(T)/\kappa_N(T)$ as $T\rightarrow T_c$ of about 1.6 for a pure sample. This is a little less than the value of 1.82 we find for a pure superconductor. The discrepancy is not too surprising since Sn is not truly a weak-coupling superconductor. Also the samples studied in Ref. 3 are never really pure. Estimates of c from the ratio of the room-temperature resistance to the residual resistance for the cleanest sample studied in Ref. 3 result in $c \gtrsim 1.5$. This means, as discussed in the preceding section, that $\kappa_s(T)/\kappa_N(T_c)$ should decrease as the temperature is lowered below T_c, which indeed is observed. The experiments also show that there are small deviations from Matthiessen's rule in the normal state. An inherent limitation in comparing the theory presented here with experiment is the assumption of an isotropic model. Pure tin is known to have pronounced band-structure anisotropies, but as discussed in Ref. 3 an average of $\kappa_s(T)$ over all directions gives good agreement with the theory for isotropic models.

Mezahov-Deglin[18] measured κ_s in pure lead for temperatures below T_c, and obtained results for κ_s which look very much like curves A and B in Fig. 7. However, Mezahov-Deglin[18] analyzed the behavior of κ_s for $T/T_c \lesssim 0.7$ in terms of lattice conduction. The behavior for $0.3 \lesssim T/T_c \lesssim 0.7$ was explained as lattice conduction with the mean free path of phonons being limited by scattering from the quasiparticles. The increase in κ_s as temperature decreases is then due to the decrease of the number of quasiparticles. Below the maximum, the mean free path of the phonons is determined by the sample size, so the ultimate dependence should be $\kappa_s \propto T^3$ at very low temperatures.

The results in the preceding section show that the maximum in heat conductivity may be explained in terms of the electronic contribution. We are not able to make a detailed comparison with experiment[18] since the impurity scattering rate $\tau_{\rm imp}^{-1}$ cannot be estimated from the available experimental data. This is basically due to the uncertainty in determining κ_N when the magnetic field is zero. The version of Kohler's rule used in Ref. 18 gives a value of the ratio of the room-temperature resistance to the residual resistance of 10^5, which corresponds to $c \simeq 0.06$. However, as discussed in Ref. 18 another version of Kohler's rule would result in a smaller value of c, which is necessary if the larger maximum in κ_s is explained in terms of electronic heat conduction.

Recently, Odoni *et al.*[27] measured the thermal conductivity of pure lead in the temperature range $0.007 < T/T_c < 0.17$. They showed that the thermal conductivity within this temperature range is due to lattice conduction, since they observed the size dependence of κ_s and verified the dependence $\kappa_s \propto T^3$, except at the lowest temperatures. Unfortunately, their measurements did not extend to high enough temperatures to allow comparison with our calculations of the electronic contribution.

IV. CHARGE IMBALANCE

It is often useful in describing properties of superconductors to separate the total current into a normal current associated with the excitations, and a supercurrent associated with the moving condensate. In a similar spirit, one may express the total charge as a contribution from the distribution of excitations, and a contribution from the condensate. The two contributions are referred to as the charge of the normal component and the charge of the superconducting component, respectively, and form the basis for the development of a two-fluid model for the charge density, as described in detail by Pethick and Smith.[12,28]

The total charge density is given by (2.66). In the situations that interest us here, the changes in the total charge are suppressed by Coulomb interactions, that is $\delta\rho=0$. In nonequilibrium situations, the system then responds by setting up a potential ϕ, which is seen from (2.66) to be given by

$$e\phi = \int dE \frac{d\Omega_{\hat{p}}}{4\pi}(N_1^2 - R_2^2)\delta f \equiv \frac{Q^*}{2N(0)} , \tag{4.1}$$

which defines the quasiparticle charge Q^*. The expression (4.1) for Q^* is identical with that of Ref. 16, Eq. (A22), since $N_1 f^T = (N_1^2 - R_2^2)\delta f$ according to (2.33). The

charge imbalance Q^* is then detected by measuring a voltage across a detector junction when no current flows through it. The voltage detected is

$$V_d=\frac{\phi}{g_{NS}}=\frac{Q^*}{2eN(0)g_{NS}}\ , \tag{4.2}$$

where

$$g_{NS}=\int dE N_1\left[-\frac{\partial f^0}{\partial E}\right] \tag{4.3}$$

is the normalized tunneling conductance, as discussed, for example, in Ref. 12.

A. Charge imbalance generated by tunnel injection

In the tunnel-injection experiments pioneered by Clark,[29] a quasiparticle current is injected, via a tunnel junction, from a normal metal (N) into a superconductor (S). Here it is converted into a supercurrent which flows out of the active volume. The volume has been chosen so that the deviation from equilibrium is constant in space. In steady state, with the quasiparticle charge injected at a rate dQ_i^*/dt, the excess distribution relaxes at a rate $\tau_{Q^*}^{-1}$ to produce a steady-state charge imbalance Q^*,

$$\frac{dQ_i^*}{dt}=\frac{Q^*}{\tau_{Q^*}}\ , \tag{4.4}$$

which defines τ_{Q^*}. The voltage detected in a tunnel injection experiment is then, according to (4.2), proportional to τ_{Q^*}.

Schmid[30] has shown how the injection of quasiparticles from the normal metal at voltage V is included in the quasiclassical Green-function approach. Assuming that the normal metal is in equilibrium and going to second order in the tunneling Hamiltonian, Schmid[30] finds the following contributions to the self-energy:

$$\begin{aligned}\Sigma_T^{R\,(A)}&=\mp i\pi N_N(0)\,|\,T_{NS}\,|^2\tau_3\ ,\\ \Sigma_T^K&=-i2\pi N_N(0)\,|\,T_{NS}\,|^2\tau_3\tanh\left[\frac{E-eV\tau_3}{2T}\right]\ ,\end{aligned} \tag{4.5}$$

where T_{NS} is the tunneling matrix element, and $N_N(0)$ is the density of states per spin at the Fermi surface of the normal metal. The kinetic equation (2.58) takes the form

$$0=I_{\rm ph}+I_{\rm imp}+I_s+I_T\ , \tag{4.6}$$

where

$$\begin{aligned}I_T=2\pi N_N(0)\,|\,T_{NS}\,|^2\Bigg\{&\frac{N_1^2-R_2^2}{2}[f^0(E-eV)-f^0(E+eV)]\\&-\frac{N_1}{4}\left[\tanh\left[\frac{E+eV}{2T}\right]+\tanh\left[\frac{E-eV}{2T}\right]-2(1-2f)\right]\Bigg\}\ .\end{aligned} \tag{4.7}$$

In the situations we consider here the nonequilibrium contribution to the injected charge is small compared with the total, so we neglect it in (4.7) as was done in Ref. 12. Since quasiparticle charge is determined by the part of δf even in E, we only need to retain the even part of I_T which acts as a driving term in the kinetic equation. In the spatially homogeneous case, we have

$$\pi N_N(0)\,|\,T_{NS}\,|^2[f^0(E+eV)-f^0(E-eV)](N_1^2-R_2^2)=I_{\rm ph}+I_{\rm imp}+I_s\ . \tag{4.8}$$

The collision integrals are most conveniently discussed in terms of the deviation function ψ defined by $f=f^0+f^0(1-f^0)\psi$, and we find the following.

(1) Phonons: From the Appendix, we have

$$I_{\rm ph}(\psi)=\frac{-1}{4\cosh^2(E/2T)}\int_{-\infty}^{\infty}dE'B(E',E)\left[(N_1N_1'-R_2R_2')\psi(E)-(N_1^2-R_2^2)(N_1'^2-R_2'^2)\left[1+\frac{N_2N_2'}{N_1N_1}\right]\psi(E')\right]\ , \tag{4.9}$$

where the function $B(E,E')$ is defined by (2.44).

(2) Impurities: From the Appendix, we find

$$I_{\rm imp}(\psi)=0 \tag{4.10}$$

as long as the system is isotropic. The impurities do not relax the quasiparticle charge because they scatter on constant energy surfaces, which do not change the isotropic δf. The magnetic impurities contribute according to the Appendix:

$$I_s(\psi)=-\frac{1}{\tau_s}\{N_1^2+R_2^2-(N_1^2-R_2^2)^2[1-(N_2/N_1)^2]\}\frac{\psi(E)}{4\cosh^2(E/2T)}\ . \tag{4.11}$$

The full kinetic equation is then

$$4\pi N_N(0)\,|\,T_{NS}\,|^2[f^0(E+eV)-f^0(E-eV)]\cosh^2\frac{E}{2T}(N_1^2-R_2^2)$$
$$=-\left[\frac{N_1^2+R_2^2-(N_1^2-R_2^2)^2[1-(N_2/N_1)^2]}{\tau_s}+\int_{-\infty}^{\infty}dE'B(E',E)(N_1N_1'-R_2R_2')\right]\psi(E)$$
$$+\int_{-\infty}^{\infty}dE'B(E',E)(N_1^2-R_2^2)(N_1'^2-R_2'^2)\left[1+\frac{N_2N_2'}{N_1N_1'}\right]\psi(E')\,, \tag{4.12}$$

where the generalized densities of states are obtained from the same quartic equation (2.53) as for thermal conductivity.

To demonstrate the equivalence of the quasiparticle Boltzmann equation and Eq. (4.12) in the weak pair-breaking limit, we have to retain first-order terms of pair-breaking rates associated with electron-phonon and spin-flip scattering, which corresponds to the use of the generalized densities of states (3.12)–(3.15). Equation (4.12) then reduces to the quasiparticle Boltzmann equation discussed by, for example, Pethick and Smith[12,28] and Chi and Clarke.[15] In Ref. 16 we used the distribution functions introduced by Schmid and Schön,[9] and to show the equivalence between the two approaches, we had to expand $\mathrm{Re}ZN_2$ and $\mathrm{Re}\Phi_1N_2$ in the pair-breaking rates.

The charge-relaxation rates have been calculated for arbitrary temperatures, within the quasiparticle approach, by Chi and Clarke[15] and by Lemberger and Clarke.[31] Lemberger and Clarke[31] found that the experimental data they obtained were fitted very well by an interpolation formula derived by Schmid and Schön,[9]

$$\tau_{Q^*}^{-1}=\frac{\pi}{4}\frac{\Delta}{T}\left[\frac{1}{\tau_{\mathrm{in}}}\left[\frac{1}{\tau_{\mathrm{in}}}+\frac{2}{\tau_s}\right]\right]^{1/2}, \tag{4.13}$$

valid in the region $\Delta/T\ll 1$ and $\tau_s^{-1}\ll(T/\Delta)^2\tau_{\mathrm{in}}^{-1}$. The numerical solution of the quasiparticle Boltzmann equation only gives the result (4.13) in a very small temperature region near T_c [except for small corrections discussed below Eq. (47) in Ref. 16], while the calculated relaxation rates at lower temperatures are significantly higher and do not follow the simple universal dependence on $\tau_{\mathrm{in}}/\tau_s$ implied by (4.13). In Ref. 16 the full effects of pair breaking were studied within the Green-function approach, and compared with the results obtained from the quasiparticle Boltzmann equation for the temperatures and injection voltages of experimental interest. The result obtained in Ref. 16 showed that the solution of the full kinetic equation for the parameters investigated is much closer to the solution of the quasiparticle Boltzmann equation than to the extrapolated Schmid and Schön[9] formula, except for $\Delta/T\ll 1$. The temperature dependence of Q^* and τ_{Q^*} at low temperatures and for low injection voltage is found by introducing the variable $\xi=\mathrm{sgn}E(E^2-\Delta^2)^{1/2}$ in the kinetic equation and then scale the energy to $(\Delta T)^{1/2}$. The result is that $Q^*\propto(\Delta/T)^3e^{-\Delta/T}$ for $T/\Delta\ll 1$. The injected quasiparticle charge per unit time has a temperature dependence given by

$$\frac{dQ_i^*}{dt}\propto(T/\Delta)^{-1/2}e^{-\Delta/T}\,,$$

so

$$\tau_{Q^*}=\frac{Q^*}{dQ_i^*/dt}\propto T^{-5/2}\,, \tag{4.14}$$

in agreement with the result in Ref. 32.

We have solved Eq. (4.12) within the model for pure lead discussed in the previous chapter.[17] In Fig. 13 we plot the calculated charge-relaxation rate at the constant injection voltage eV equal to ten times the $T=0$ energy gap $\Delta(0)$. The dashed curve is the charge-relaxation rate for a pure weak-coupling superconductor within the Debye model. In both cases, the rate has been normalized to the τ_{in}^{-1} obtained from the two different effective phonon density of states α^2F. Close to T_c, both curves follow the result $\tau_{Q^*}^{-1}=(\pi\Delta/4T)\tau_{\mathrm{in}}^{-1}$, while the strong-electron-phonon coupling in lead leads to a larger charge-relaxation rate than in weak-coupling superconductors at lower temperatures. A comparison with the measurements of Clarke and Paterson[33] shows that the calculated value of τ_{Q^*} at $T=0.6T_c$ is 30% larger than the measured value. The calculation shows a fast rise in τ_{Q^*} at lower temperatures, much faster than observed in the experiment. This may be due to the approximation that the gap is isotropic, which prevents charge relaxation from the impurities. Tomlinson and Carbotte[34] have calculated the mean-square gap anisotropy with the result

$$\frac{\langle\Delta_{\vec{p}}^2\rangle-\langle\Delta_{\vec{p}}\rangle^2}{\langle\Delta_{\vec{p}}^2\rangle}\simeq 10^{-2}$$

at $T=0$, where the angular brackets denote an angular average. This has to be included in the calculations to make comparison with experiment at low temperatures meaningful.

As discussed in Sec. III B, the main problem in treating

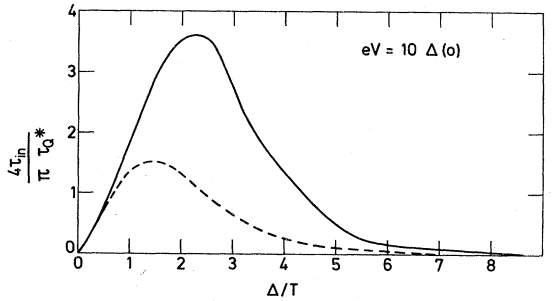

FIG. 13. Plot of quantity $4\tau_{\mathrm{in}}/\pi\tau_{Q^*}$ as a function of Δ/T. The dashed curve shows the result for a weak-coupling superconductor, while the solid curve shows the result for lead. In the strong-coupling case, Δ is the value of the real part of the gap function Φ_1/Z at the gap edge.

strong-coupling superconductors is to solve the Eliashberg equations. The results for thermal conductivity suggest that it is possible to obtain reasonable results by neglecting the broadening of energy levels, that is, we use the density of states (3.12)—(3.15) with the gap following (3.19) and keep the model form for α^2F. The numerical calculations show that this quasiparticle approximation is within 10% of the exact result for all temperatures.

V. CONCLUSIONS

In the previous sections we have demonstrated how the quasiclassical Green-function approach to nonequilibrium superconductivity may be used to make realistic calculations of the charge-relaxation rate and the thermal resistivity of strong-coupling materials such as Pb. The important frequency dependence of the effective phonon density of states α^2F was taken fully into account. However, our model does not include any explicit effects of band anisotropy. The pronounced differences between weak- and strong-coupling superconductors are mainly due to the frequency dependence of the effective phonon density of states, while the effects of broadening play a relatively minor role. Our detailed study of Pb suggests that calculations for other materials may be performed in a quasiparticle approximation, which neglects broadening but takes into account the frequency dependence of the effective phonon density of states in the quasiparticle collision integral.

APPENDIX

In this appendix we give expressions for the collision integrals for each scattering mechanism separately, obtained from the self-energy expressions (2.34)—(2.37). We first consider the phonons and obtain

$$I_{\rm ph}=-\frac{1}{8i}\mathrm{tr}\{P_1^R[(\Sigma_{\rm ph}^R-\Sigma_{\rm ph}^A)F_1-\Sigma_{\rm ph}^K]P_1^A\}$$

$$=-2\pi N(0)\sum_\mu\int dx\,dy\frac{d\Omega_{\hat p'}}{4\pi}|g^\mu_{\vec p'-\vec p}|^2\rho_\mu(\vec p'-\vec p,y)\delta(y-x+E)$$

$$\times\{[K_1(\hat p,\hat p',x,E)+K_2(\hat p,\hat p',x,E)][N(y)+f^0(\hat p',x)]\delta f(\hat p,E)$$

$$-[N(y)+f^0(-\hat p,-E)][K_1(\hat p,\hat p',x,E)\delta f(\hat p',x)-K_2(\hat p,\hat p',x,E)\delta f(-\hat p',-x)]\}\ , \tag{A1}$$

The contribution from the nonmagnetic impurities are obtained from Eq. (2.34),

$$I_{\rm imp}=-\frac{1}{8i}\mathrm{tr}\{P_1^R[(\Sigma_1^R-\Sigma_i^A)F_1-\Sigma_i^K]P_1^A\}$$

$$=-\frac{1}{\tau_{\rm imp}}\int\frac{d\Omega_{\hat p'}}{4\pi}w(\hat p\cdot\hat p')\{[K_1(\hat p,\hat p',E,E)+K_2(\hat p,\hat p',E,E)]\delta f(\hat p,E)$$

$$-[K_1(\hat p,\hat p',E,E)\delta f(\hat p',E)-K_2(\hat p,\hat p',E,E)\delta f(-\hat p',-E)]\}\ , \tag{A2}$$

and finally the contribution from the magnetic impurities is obtained from (2.35)

$$I_s=-\frac{1}{8i}\mathrm{tr}\{P_1^R[(\Sigma_s^R-\Sigma_s^A)F_1-\Sigma_s^K]P_1^A\}$$

$$=-\frac{1}{\tau_s}\int\frac{d\Omega_{\hat p'}}{4\pi}w_s(\hat p\cdot\hat p')\{[K_3(\hat p,\hat p',E,E)+K_4(\hat p,\hat p',E,E)]\delta f(\hat p,E)$$

$$-[K_3(\hat p,\hat p',E,E)\delta f(\hat p',E)-K_4(\hat p,\hat p',E,E)\delta f(-\hat p',-E)]\}\ . \tag{A3}$$

The coherence factors K_1, K_2, K_3, and K_4 entering the collision integrals are listed below in terms of the generalized densities of states. We use the notation that functions of $(\hat{p}',x)$ have a tilde, for example, $N_1(\hat{p}',x)=\tilde{N}_1$, while, for example, $N_1(\hat{p},E)=N_1$,

$$K_1(\hat{p},\hat{p}',x,E)=\tfrac{1}{16}\mathrm{tr}(P_1^R\tilde{P}_1^R\tilde{P}_1^A P_1^A)$$
$$=\frac{1}{2}\left[N_1\tilde{N}_1-R_2\tilde{R}_2+(N_1^2-R_2^2)\times(\tilde{N}_1^2-\tilde{R}_2^2)\left[1+\frac{N_2\tilde{N}_2}{N_1\tilde{N}_1}\right]\right], \quad \text{(A4)}$$

$$K_2(\hat{p},\hat{p}',x,E)=-\tfrac{1}{16}\mathrm{tr}(P_1^R\tilde{P}_2^R\tilde{P}_2^A P_1^A)$$
$$=\frac{1}{2}\left[N_1\tilde{N}_1-R_2\tilde{R}_2-(N_1^2-R_2^2)\times(\tilde{N}_1^2-\tilde{R}_2^2)\left[1+\frac{N_1\tilde{N}_1}{N_2\tilde{N}_2}\right]\right]. \quad \text{(A5)}$$

The coherence factors K_3 and K_4 entering the collision integral from magnetic impurities are

$$K_3(\hat{p},\hat{p}',E,E)=\tfrac{1}{16}\mathrm{tr}(P_1^R\tau_3\tilde{P}_1^R\tilde{P}_1^A\tau_3P_1^A)$$
$$=\frac{1}{2}\left[N_1\tilde{N}_1+R_2\tilde{R}_2+(N_1^2-R_2^2)\times(\tilde{N}_1^2-\tilde{R}_2^2)\left[1-\frac{N_2\tilde{N}_2}{N_1\tilde{N}_1}\right]\right] \quad \text{(A6)}$$

and

$$K_4(\hat{p},\hat{p}',E,E)=-\tfrac{1}{16}\mathrm{tr}(P_1^R\tau_3\tilde{P}_2^R\tilde{P}_2^A\tau_3P_1^A)$$
$$=\frac{1}{2}\left[N_1\tilde{N}_1+R_2\tilde{R}_2-(N_1^2-R_2^2)\times(\tilde{N}_1^2-\tilde{R}_2^2)\left[1-\frac{N_2\tilde{N}_2}{N_1\tilde{N}_1}\right]\right]. \quad \text{(A7)}$$

[1] J. Bardeen, G. Rickayzen, and L Tewordt, Phys. Rev. **113**, 982 (1959).
[2] J. H. P. Watson and G. M. Graham, Can. J. Phys. **41**, 1738 (1963).
[3] A. M. Guénault, Proc. R. Soc. London Ser. A **204**, 420 (1961).
[4] V. Ambegaokar and L. Tewordt, Phys. Rev. **134**, **A805** (1964).
[5] V. Ambegaokar and J. Woo, Phys. Rev. **139**, **A1818** (1965).
[6] G. Eilenberger, Z. Phys. **214**, 195 (1968).
[7] G. M. Eliashberg, Zh. Eksp. Teor. Fiz. **61**, 1254 (1971) [Sov. Phys.—JETP **34**, 668 (1972)].
[8] A. I. Larkin and Yu. N. Ovchinnikov, Zh. Eksp. Teor. Fiz. **55**, 2262 (1968) [Sov. Phys.—JETP **28**, 1200 (1969)]; Zh. Eksp. Teor. Fiz. **73**, 299 (1977) [Sov. Phys.—JETP **46**, 155 (1977)].
[9] A. Schmid and G. Schön, J. Low Temp. Phys. **20**, 207 (1975).
[10] A. G. Aronov and V. L. Gurevich, Fiz. Tverd. Tela **16**, 2656 (1974) [Sov. Phys.—Solid State **16**, 1722 (1974)].
[11] O. Betbeder-Matibet and P. Nozières, Ann. Phys. (N.Y.) **51**, 392 (1969).
[12] C. J. Pethick and H. Smith, Ann. Phys. (N.Y.) **119**, 113 (1979).
[13] A. L. Shelankov, Zh. Eksp. Teor. Fiz. **78**, 2359 (1980) [Sov. Phys. —JETP **51**, 1186 (1980)].
[14] M. Tinkham, Phys. Rev. B **6**, 1747 (1972).
[15] C. C. Chi and J. Clarke, Phys. Rev. B **19**, 4495 (1979); **21**, 333 (1980).
[16] J. Beyer Nielsen, C. J. Pethick, J. Rammer, and H. Smith, J. Low Temp. Phys. **46**, 565 (1982).
[17] J. Beyer Nielsen and H. Smith, Phys. Rev. Lett. **49**, 689 (1982).
[18] L. P. Mezahov-Deglin, Zh. Eksp. Teor. Fiz. **77**, 733 (1979) [Sov. Phys.—JETP **50**, 369 (1979)].
[19] J. Beyer Nielsen, Ph.D. thesis, University of Copenhagen, 1983.
[20] L. V. Keldysh, Zh. Eksp. Teor. Fiz. **47**, 1515 (1964) [Sov. Phys.—JETP **20**, 1018 (1965)].
[21] J. S. Langer, Phys. Rev. **128**, 110 (1962).
[22] D. J. Scalapino, in *Superconductivity,* edited by R. D. Parks (Dekker, New York, 1969), p. 445; see also case 2, p. 532.
[23] J. M. Rowell, W. L. McMillan, and W. L. Feldman, Phys. Rev. **178**, 897 (1969).
[24] L. Tewordt, Phys. Rev. **129**, 657 (1963).
[25] W. L. McMillan and J. M. Rowell, in *Superconductivity,* edited by R. D. Parks (Dekker, New York, 1969), p. 561.
[26] *Thermal Conductivity of Solids at Room Temperature and Below,* edited by G. E. Childs, L. J. Ericks, and R. L. Powell, Natl. Bur. Stand. (U.S.) Mongoraph No. 131 (U.S. GPO, Washington, D.C., 1973).
[27] W. Odoni, P. Fuchs, and H. R. Ott, Phys. Rev. B **28**, 1314, (1983).
[28] C. J. Pethick and H. Smith, J. Phys. C **13**, 6313 (1981).
[29] J. Clarke, Phys. Rev. Lett. **28**, 1363 (1972).
[30] A. Schmid, in *Proceedings of the NATO Advanced Study Institute,* edited by K. E. Gray (Plenum, New York, 1981), p. 423.
[31] T. R. Lemberger and J. Clarke, Phys. Rev. B **23**, 1088 (1981); **23**, 1100 (1981).
[32] U. Eckern and G. Schön, J. Low Temp. Phys. **32**, 821 (1978).
[33] J. Clarke and J. L. Paterson, J. Low Temp. Phys. **15**, 491 (1974).
[34] P. G. Tomlinson and J. P. Carbotte, Phys. Rev. B **13**, 4738 (1976).